We are IntechOpen, the world's leading publisher of Open Access books Built by scientists, for scientists

6,900
Open access books available

186,000
International authors and editors

200M
Downloads

Our authors are among the

154
Countries delivered to

TOP 1%
most cited scientists

12.2%
Contributors from top 500 universities

CLARIVATE ANALYTICS
BOOK CITATION INDEX
INDEXED

WEB OF SCIENCE™

Selection of our books indexed in the Book Citation Index
in Web of Science™ Core Collection (BKCI)

Interested in publishing with us?
Contact book.department@intechopen.com

High-Energy Nanosecond Laser Pulses for Synthesis of Better Bone Implants

Amirkianoosh Kiani and Mitra Radmanesh

Additional information is available at the end of the chapter

http://dx.doi.org/10.5772/63770

Abstract

The main objective of this chapter is to introduce high-energy nanosecond laser pulse treatment for enhancing the surface bioactivity of titanium for bone and tissue implant fabrication. Improvement to the implant performance could immensely benefit the human patient. Bioactivity enhancement of materials is currently an essential challenge in implant engineering. Laser micro/nano surface texturing of materials offers a simple, accurate, and precise method to increase the biocompatibility of materials in one single step. In this chapter, the effects of laser power, scanning parameters, and frequency on surface structure and topographic properties are studied. Through bioactivity assessment of treated titanium substrates, it was found that an increase in power and frequency increases the bioactivity of titanium, while a decrease in scanning speed of laser could lead to an increase in the cell adhesion ability of titanium.

Keywords: titanium, bone implant, laser surface treatment, micro- and nanotexturing, bioactivity, biocompatibility

1. Introduction: biomaterials and implant engineering

Biomaterials and implant engineering have become vital fields in the medical and surgical industries. These disciplines can enhance the quality and length of human life, and have an immense effect on the health of numerous individuals. The technologies associated with biomaterials and implant engineering, particularly in the fields of surgical implants such as dental, bone, and tissue implant applications, have led to the creation of numerous research opportunities [1–3]. In today's society, with the continuous growth in population and education, there is a preference for an improved lifestyle, better body functionality, and more appealing

aesthetics. This leads to ongoing expansion and discovery in the technology and science associated with biomaterials and implant engineering [3–6].

This chapter describes a research opportunity for the investigation and improvement of the effects of laser surface texturing on enhancing the biocompatibility and bioactivity of titanium. Titanium substrates are used to examine the effects of key laser process parameters, including power, scanning parameters, and frequency on their surface topography properties and biocompatibility.

1.1. Main challenge in implant engineering

Cell adhesion and biocompatibility are important parameters for implant fabrication and the production of biomedical devices. Improvements to an implant's performance in the implantation site could benefit the patient's quality of life. Low biocompatibility is often caused by poor integration of the implant with surrounding tissues. Cell behaviour on biomaterial surfaces depends upon implant-cell interactions, which are correlated with surface properties such as hydrophilicity, roughness, texture, chemical composition, charge, and topography properties [6–8]. Although there is a great range in the design and function of various implants, the one common factor for all of them is their biocompatibility, which affects overall implant performance. Biocompatibility enhancement of materials used in implants is currently an essential challenge in implant engineering [8]. This property is essential in order to avoid any infections and immune system rejection. It can also affect the healing process by reducing the healing time. A reduced healing time is desirable in implant applications, since the sooner the body accepts the implant organ, the sooner the user can function normally [7, 9, 10].

The implant's surface is the main area in contact with the body at an implantation site. Therefore, to increase the biocompatibility of a material, various methods of surface treatment are currently being used in industry [9, 11, 12].

1.2. Fabrication methods of biocompatible materials

One method to affect the surface properties of a material is to alter the surface topography properties. There are multiple conventional methods used commercially for processing and surface texturing of materials for bone and tissue implant applications [9, 11]. The most common mechanical methods for altering surface topography properties include sandblasting and machining, while acid etching and oxidation are common chemical methods. Although these methods are effectively used in industry, there are major disadvantages associated with them. Slow production time, complex control processes, and chemical contaminations are only a small number of the challenges presented by these commonly used processing techniques [13]. The newly developing method of laser surface texturing of materials addresses these disadvantages in a simple and effective manner. Lasers are able to deliver very low to high energy with extreme precision in dimension, spatial distribution, and temporal distribution. Lasers offer better control and precision, offer more feasibility, and are environmentally friendly [14–16]. Decreased processing time makes lasers particularly suitable for mass production, rapid prototyping, and custom-scale manufacturing for a wide variety of

applications, such as microwelding, drilling, cutting, and heat treatment of metals and alloys. Laser treatment is known for its fast and precise manner in the processing of materials, and for the variety of scales offered by lasers, including micro-, submicro-, and nanofabrication [8, 15].

1.3. Physics of laser surface texturing

Laser processing can be applied in two categories based on the energy requirements: first, applications requiring relatively low energy with limited structural and physical changes; second, applications calling for high-energy transformations for significant structural changes over a large volume, such as welding. Energy transformation in applications involving lasers requires the coupling of the laser radiation with the electrons of the interacting surface, such as metals or semiconductors [17, 18]. In return, the speed of energy transformation from the laser beam to the surface becomes fully dependent on the nature of the interacting material and its chemical bonding. There have been significant improvements in energy transformation of lasers through the development of ultrashort lasers [19–23].

Ultrashort lasers decrease the interaction time (pulse duration) between the laser and the material, which reduces the effects on the bulk material. Despite these improvements, ultrashort laser systems are relatively expensive and cannot be utilized in industries. Hence, depending on the nature of the application, less expensive yet advanced laser systems, with pulse durations in the range of nanoseconds, are more popular among manufacturers because they are more widely available in manufacturing sectors. An understanding of the laser irradiation mechanism is required to utilize the more common lasers to their fullest capability, therefore, choosing the laser parameters is essential to the final quality of a particular application [24–27].

2. Laser-enhanced topography properties

Micro/submicro-treated surfaces are popularly used in scaffold systems for bone and tissue implant applications. The surface topography properties of a material, particularly roughness, are influential on the cell adhesion rate of bone-like apatite to surfaces. Increasing the cell adhesion rate to the surface of a material increases the biocompatibility of the material. Thus, surface texturing of materials to enhance their biocompatibility is effective method in the fabrication of implant devices [26–28]. The effects of laser irradiation on the surface topography properties of materials are the main advantage of laser surface texturing. Laser parameters, including frequency, power, and laser scanning parameters, can influence these material properties greatly [27].

The irradiated surface area of a material has increased surface irregularities. In return, the exposed area is more readily available for cell attachment, which enhances the apatite-inducing ability and cell adhesion rate of the material [27–31]. Furthermore, laser treatment of the materials increases the surface temperature up to oxidation temperature, and results in the creation of thin layers of oxide upon the surface. An increase in the oxidation of the surfaces

increases the wettability of surface of the material. Consequently, this leads to an increase in the apatite-inducing ability of the material and greatly improves the biocompatibility of the implant surfaces [30–35].

2.1. Laser system

The nanosecond laser used for obtaining all the results discussed in this chapter was a Nd:YAG pulsed laser system (SOL-20 by Bright Solutions Inc). The maximum output power is 20 W with a wavelength of 1064 nm and a repetition rate ranging between 10 and 100 kHz. This laser emits pulses of 6–35 ns pulse duration. The diameter of circular output beam from the laser is around 9 mm. The diameter of beam is reduced to 8mm by using an iris diaphragm before entering to galvo-scanner. A two-axis galvo-scanner (JD2204 by Sino Galvo) with the input aperture of 10 mm and beam displacement of 13.4 mm was used for beam scanning since it has a high scanning speed (to 3000 mm/s). In order to focus the normal beam to the surface of Ti, scan lens of a focal length of 63.5 mm was used. The theoretical focused laser spot diameter (d_0) is calculated to be 20 μm. During the experiment, the spot size may be bigger due to scatter and misalignment. The average laser fluence was 900 μJ at the frequency of 10 kHz.

The scanning parameters including scanning speed, and scanning configurations can be adjusted through the software operating the laser. When the combination of parameters is adjusted with this software, along with power and frequency set for laser irradiation, the desired pattern is irradiated across the surface of the selected material.

3. Effects of laser power

Power is one of the most influential laser parameters when surface treating a material. Adjusting the power increases the surface irregularities of the material and therefore enhances the topography properties of the substrate [25, 33]. In this chapter, the effects of four different powers on surface topographic and oxidation properties of titanium substrates are investigated, and the bioactivity of the treated substrates is examined through the use of simulated body fluid (SBF). Simulated body fluid (SBF), or formally known as hydroxyapatite, is a supersaturated insoluble calcium phosphate mineral, with the chemical composition of $Ca_{10}(PO_4)_6(OH)_2$. This fluid has a close similarity with human blood plasma and is the essential component of the biological hard tissues such as bones. Due to the high absorbance and catalytic properties of SBF, this fluid is commonly used to estimate the biocompatibility level of materials used in implant productions.

To treat the titanium substrates, a range of low to high average laser powers from 6 to 12W was used, while frequency and scanning speeds were kept constant in all cases. The effective number of pulses for all results was kept constant to be 25 pulses for frequency of 100 kHz [36, 37]. **Table 1** introduces the parameters used in more detail.

Average laser power (W)	Total number of laser pulses	Pulse energy (mJ) at 100 kHz	Pulse width (ns)	Total delivered energy (mJ)
6	25	0.06	35	1.5
8	25	0.08	35	2
10	25	0.10	35	2.5
12	25	0.12	35	3

Table 1. Laser parameters used in surface treating of Ti substrates.

3.1. Surface topography analysis

Once treated, there is often more available exposed surface area of the material because of the increase in surface roughness, which, in return, enhances the apatite-inducing ability and cell adhesion rate of that material. **Figure 1** displays the variation in the treated substrates using the stated powers.

Figure 1. Surface of treated titanium (A) 6 W, (B) 8 W, (C) 10 W, (D) 12 W.

Although the number of pulses delivered to each of these substrates is the same, as indicated in **Table 1**, the images shown in **Figure 1** clearly indicate different surface topography after laser treatment. With an increase in power, the energy delivered to the surface of the material increases as well, hence, more ablation and topography changes occur. Substrates treated with a power of 12 W have a larger surface affected by laser irradiation as opposed to 6 W.

During laser irradiation, a plasma plume with radial surface tension is formed surrounding the irradiated area due to the high temperature gradient caused by laser energy transfer. Immediately following irradiation, a high temperature difference exists between the surface of the material and the generated plasma plume. Thus, a high cooling rate results, which causes rapid re-solidification of the ablated material. Consequently, the tension within the laser plume

causes shooting of the molten titanium to outside of the ablated zones [37]. The micro re-solidified particles observed outside the crater in **Figure 1** have been formed due to the same reason.

Using 3D microscopy, the surface profile of the treated substrates can be compared; this is introduced in **Figure 2**. This study used the Zeta-20 optical profiler to scan the surface of the samples in order to obtain the surface topography results across each sample.
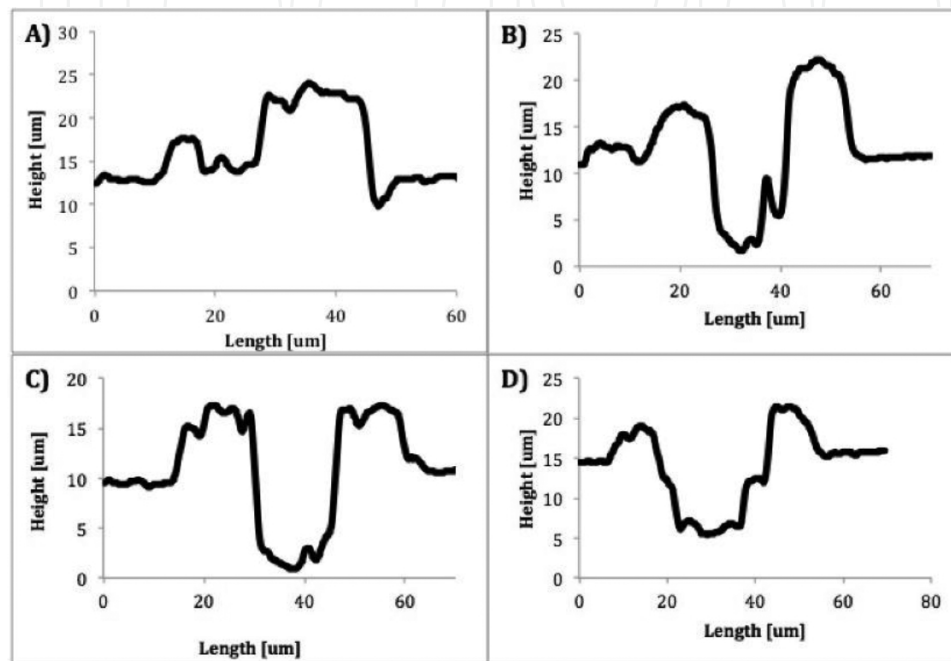

Figure 2. Surface profiles of Ti (A) 6 W, (B) 8 W, (C) 10 W, (D) 12 W.

As shown, an increase in laser power clearly affects the surface topography profile of titanium substrates. Different laser powers create different surface irregularities across the surface of the treated titanium substrates.

3.2. Surface temperature analysis

Different power levels deliver various amounts of energy to the surface of the substrate, and, therefore, increase the surface temperature of the titanium. This increase in the surface temperature could affect the surface structure, topographic properties, and oxidation of the titanium substrates. Oxidation is an important factor when considering bioactivity of a material. With higher oxidation, a higher surface energy is present, which results in more interaction between the implant and the body. Therefore, generating larger amounts of titanium oxide across the surface substrates consequently increases the biocompatibility of the treated work pieces. However, after a certain power threshold, the energy delivered to the surface of the titanium increases the surface temperature beyond the oxidation limit. Therefore, the material develops less titanium oxide as the surface undergoes larger ablation [32, 34, 38].

In order to calculate the surface temperature in this chapter, a theoretical calculation has been conducted according to the previous published results [25, 36, 39]; in this method, we assumed that the laser energy is absorbed in a much thinner layer compared to the penetration depth of the heat wave. Finally, the average surface temperature of the Ti substrate can be obtained as fully discussed in [25, 39]:

$$T_n = 2\alpha \frac{\left[1 - \frac{2}{3}\alpha\right]}{(1 + \alpha^2)} \frac{T_m}{(1 - \alpha)} \left[1 + \frac{\alpha^n - \alpha}{n(1 - \alpha)}\right] \tag{1}$$

where T_m is the maximum temperature calculated at the end of first pulse, n is the pulse numbers, and α is the constant ratio for the previous maximum and the following minimum temperatures and equal to $\alpha = (t_p/t_{pp})^{1/2}$, where t_{pp} is the pulse interval and equal to $t_{pp} = 1/f$ (f is pulse repetition rate) and t_p is pulse duration. The analytical results obtained in this study are associated with possible errors due to multiple assumptions made throughout the study.

Upon completion of the analytical analysis, the temperature profile for both cases with 8 and 10 W powers, and a pulse number range of 2 pulses to 50 pulses is obtained.

The trend of average surface temperature of the treated titanium substrates is shown in **Figure 3**.
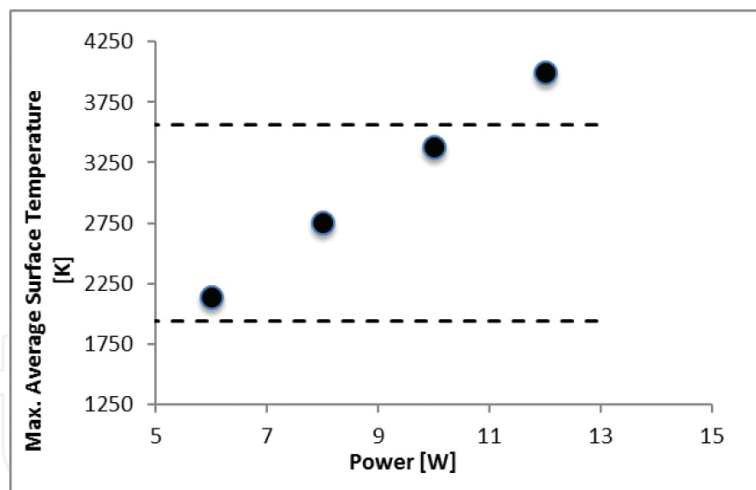

Figure 3. Maximum average surface temperature in each power.

As evident, with 12 W of power, the maximum average surface temperature of the titanium exceeds its evaporation point, and therefore less concentration of titanium oxide is generated along the surface of the substrates. Also, more ablation occurs, which agrees with the observations. Having a larger concentration of titanium oxide across the surface results in better cell interactions. To further investigate the oxidation of treated substrates, energy dispersive X-ray (EDX) analysis was conducted to detect the amount of oxygen available across the surface of substrates treated using the stated powers.
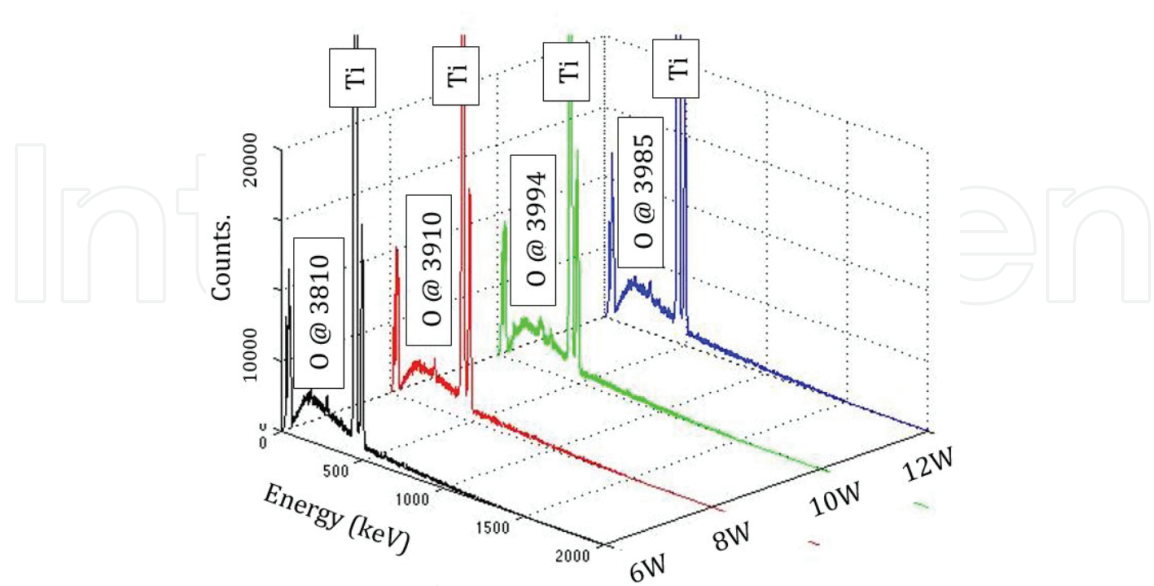
Figure 4 indicates the results.

Figure 4. EDX analysis of the irradiated Ti at 6, 8, 10, and 12 W.

Comparing the trace of oxygen across the surface of all four substrates, it is observed that with an increase in power, the oxygen concentration increases slightly as well, until a power of 12 W is reached, which shows slightly a lower trace of oxygen. This is in agreement with the average temperature results observed in **Figure 3**. Considering the results shown in **Figures 4** and **5**, it is expected that powers of 8 and 10 W would result in a better biocompatibility compared to other two powers. This conclusion is assessed through the use of simulated bodily fluids (SBF).
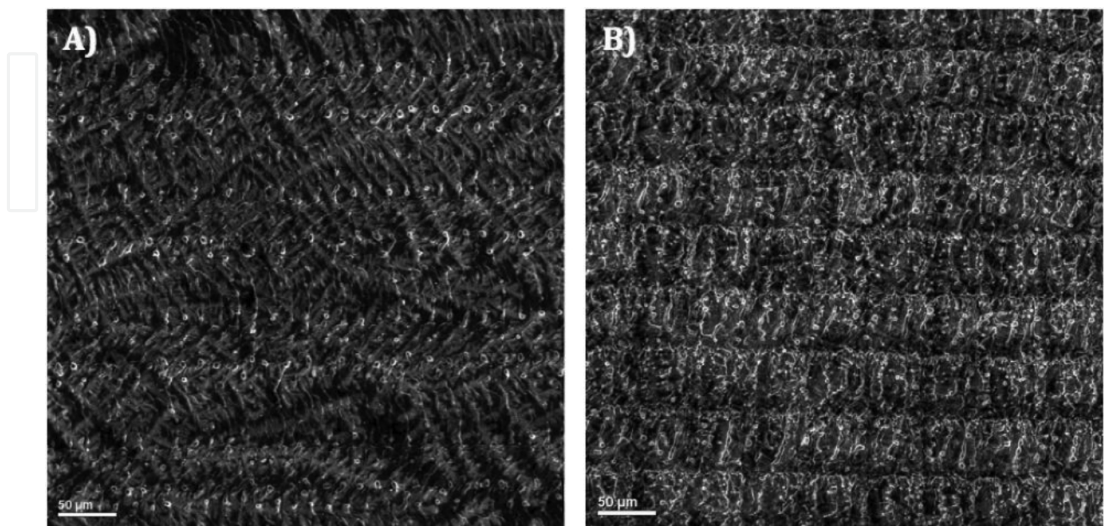

Figure 5. SBF-soaked substrates. (A) 8 W, (B) 10 W.

3.3. Biocompatibility assessment

To determine how the differences in surface topography affect the biocompatibility of titanium, the treated substrates using powers of 8 and 10 W were immersed in SBF for 7 days. **Figure 5** shows the scanning electron microscopy (SEM) photographs of the substrates after the completion of the assessment.

In **Figure 5**, the white layers across the induced line patterns indicate the bone-like apatite deposition on the surface of the titanium. These microscopy images show that generally with an increase in power, apatite-inducing ability across the surface of treated titanium increases as well. Looking closely into **Figure 5**, the EDX results for 10 W curve indicate a larger amount of apatite deposition compared to the 8 W curve. This is further observed in the EDX analysis conducted on these titanium substrates shown in **Figure 6**. Detecting larger amount of oxygen, calcium, and phosphorous elements indicates a higher apatite-inducing ability for the substrates.
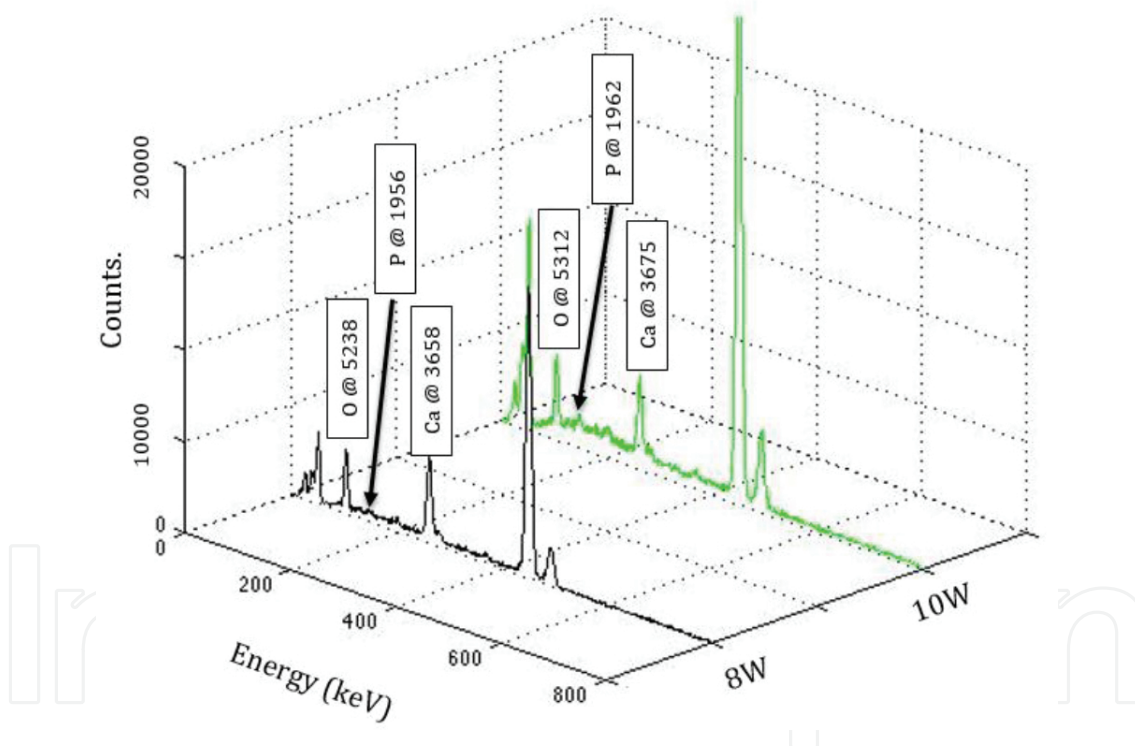

Figure 6. EDX analysis at 8 and 10 W.

As shown, the apatite-inducing ability of substrates treated with a power of 10 W is higher than the substrates treated with 8 W. This is in agreement with results observed with oxidation and SEM photography analysis.

Overall, the biocompatibility was highest for substrates treated with 10 W. This power provides adequate surface topography and the energy delivered is within the oxidation temperature range, hence creating a desirable environment for cell attachment to take place.

4. Effects of number of laser pulses

The total number of laser pulses delivered to the substrate is related to the scanning speed and laser frequency used while irradiation is taking place [40–42]. Effects of scanning speed on the number of laser pulses delivered to surface of the titanium substrates during laser irradiation are examined. Similar to power, scanning parameters have a direct effect on the surface topography and oxidation of treated titanium substrates. These effects are monitored using various scanning parameters, while keeping power and frequency constant. **Table 2** displays the parameters used.

Scanning speed (μm/ms)	Frequency (kHz)	Average power (W)	Total number of laser pulses	Total delivered energy (mJ)
50	100	10	167	16.7
200	100	10	41	4.1
400	100	10	21	2.1
500	100	10	17	1.7

Table 2. Scanning speed and pulse numbers used in surface treating of Ti substrates (pulse width, 35 ns; pulse energy, 0.1 mJ).

Scanning speed and the number of laser pulses are indirectly related. With an increase in scanning speed, the pulse number decreases. This is because with a lower scanning speed, more time is given to the laser to induce a pattern across the surface; hence, more pulses are delivered to the substrates.

4.1. Surface topography analysis

Similar to power, the effects of different scanning speeds on surface topographic properties of the treated substrates are examined using SEM photography. **Figure 7** displays these results.
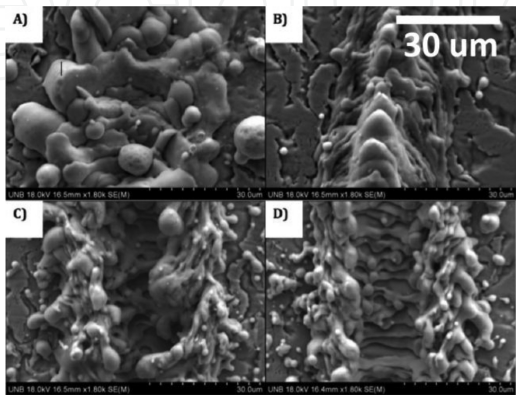

Figure 7. Surface of treated titanium (A) 50 μm/ms, (B) 200 μm/ms, (C) 400 μm/ms, (D) 500 μm/ms.

As shown in this figure, with an increase in scanning speed, the surface irregularities decrease in size; therefore, fewer topographic changes take place on those samples. This is in agreement with expectations, since **Figure 7(A)** with a scanning speed of 50 μm/ms has a larger number of pulses compared to **Figure 7(B)** with a scanning speed of 500 μm/ms.

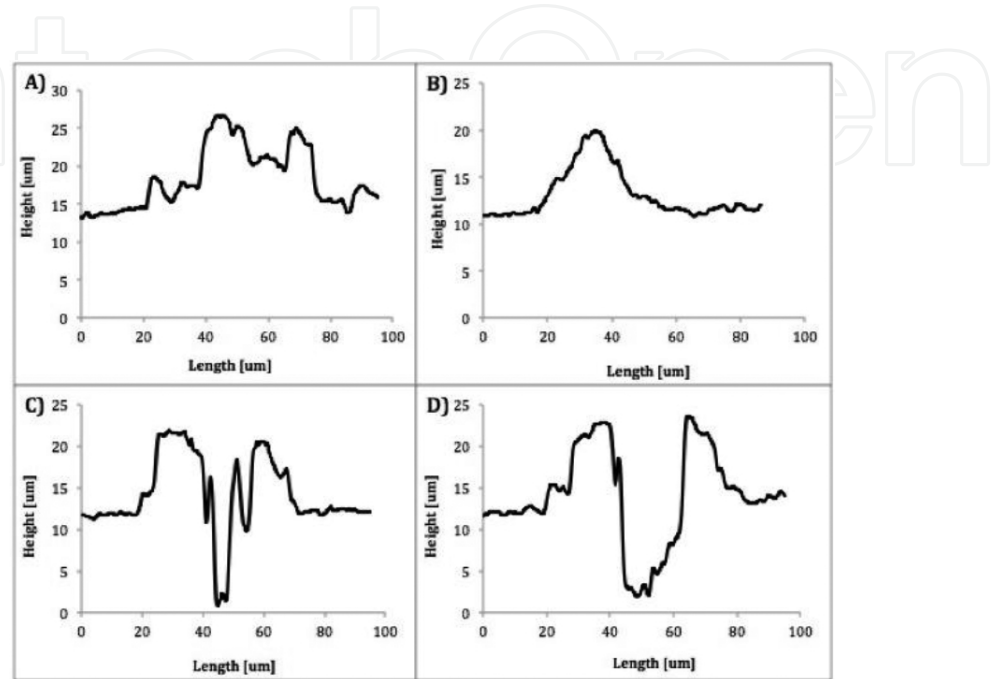The surface profile of these substrates is shown in more detail in **Figure 8**.

Figure 8. Surface profile of Ti (A) 50 μm/ms, (B) 200 μm/ms, (C) 400 μm/ms, (D) 500 μm/ms.

Figure 8(A) shows how irregularities cover the entire surface of the substrates, as opposed to only along the irradiation zone as shown in **Figure 8(D)**. This agrees with the expectations.

4.2. Biocompatibility assessment

To see how influential the number of pulses is on bioactivity enhancement of titanium, a wider range of scanning speeds is used to assess the apatite-inducing ability of treated titanium substrates. Scanning speeds of 300 and 700 μm/ms are used to treat these substrates in order to more clearly show the differences between the two substrates. All other parameters remain the same (**Table 3**).

Scanning speed (μm/ms)	Frequency (kHz)	Average power (W)	Total number of laser pulses	Total delivered energy (mJ)
300	100	10	28	2.8
700	100	10	12	1.2

Table 3. Scanning speed and pulse numbers used in surface treating of Ti substrates (pulse width, 35 ns; pulse energy, 0.1 mJ.

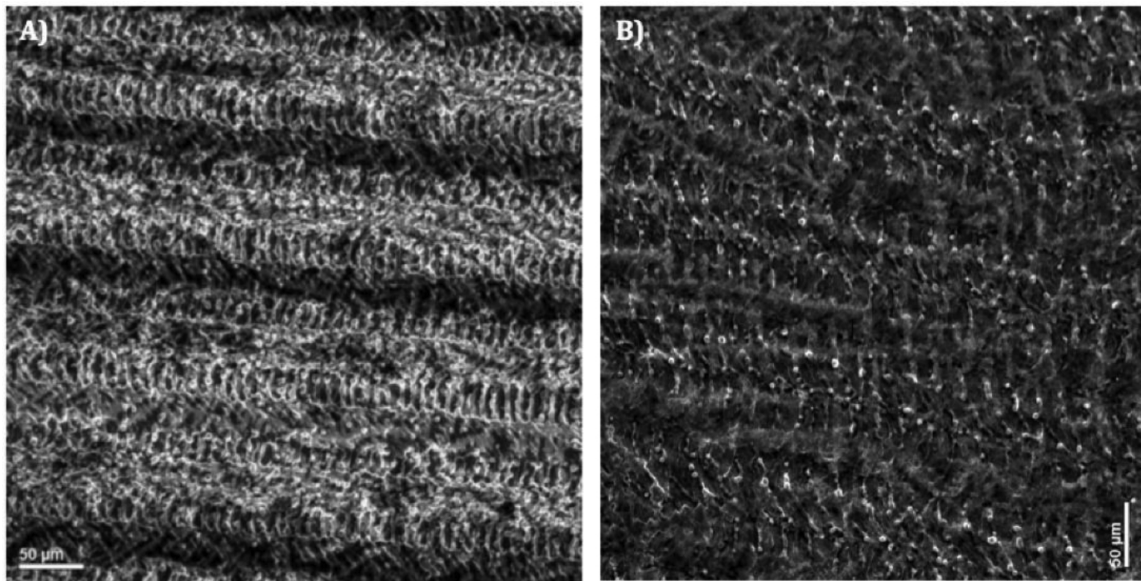**Figure 9** displays the substrates immersed in SBF for 7 days.

Figure 9. SBF-soaked substrates (A) 300 μm/ms, (B) 700 μm/ms.

As stated, a lower scanning speed delivers a larger number of pulses and therefore affects the surface topographic properties of the titanium more significantly. Additionally, with a larger number of pulses, the average surface temperature of the substrate increases, and therefore, a more ideal condition for the creation of titanium oxide is generated [25, 43]. **Figure 9** displays these effects clearly. Considering **Figure 9(A)**, more apatite deposition is observed across the surface as opposed to **Figure 9(B)**, which agrees with the expectations.

The apatite-inducing ability of these titanium substrates is further analyzed using EDX. **Figure 10** displays the results.
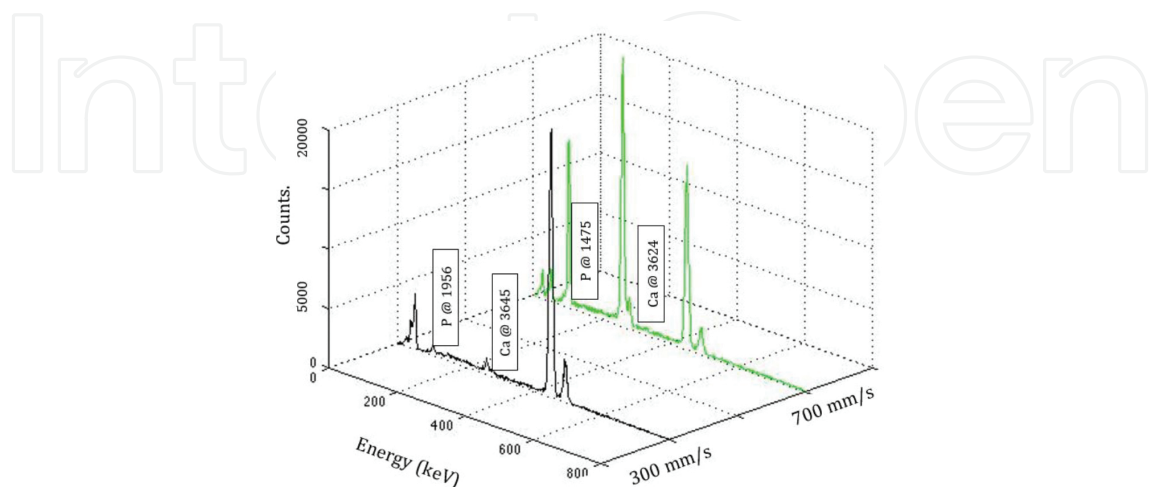

Figure 10. EDX analysis (A) 300 μm/ms, (B) 700 μm/ms.

It is evident in **Figure 10** that calcium and phosphorous concentrations detected across the surface are larger for the curve of 300 mm/s. This agrees with observations from **Figures 7** and **8**.

Overall, it was observed that with a larger number of laser pulses, more energy is delivered to the material, and therefore more surface topographic and oxidation changes take place across the surface of the treated substrates.

5. Effects of frequency

Lastly, the effects of frequency on surface of titanium substrates are examined.

A range of frequencies (25, 50, and 100 kHz) is used in surface treatment, while the average laser power and pulse width are held constant to 11 W and in the range of 15–35 nm, respectively, to ensure consistency of final results (**Table 4** introduces the parameters used in more detail).

Average laser power (W)	Laser frequency (kHz)	Pulse energy (mJ)
11	25	0.30
11	50	0.20
11	100	0.10

Table 4. Laser parameters used in surface treating of Ti substrates.

Figure 11 shows the untreated titanium substrates using laser frequencies of 25, 50, and 100 kHz.
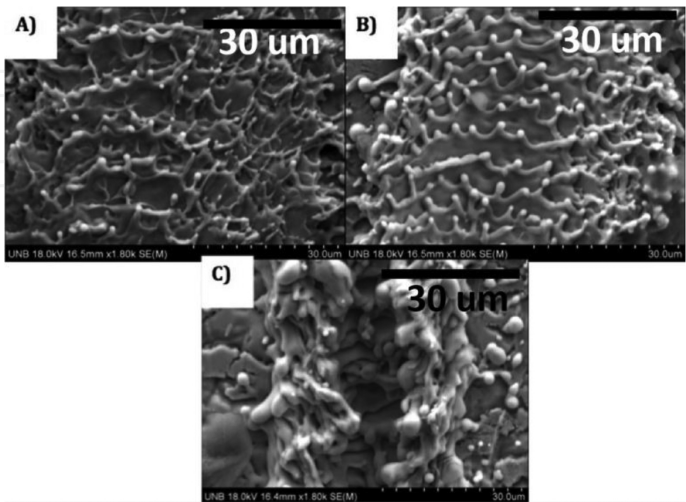

Figure 11. Non-SBF Ti substrates at laser frequency of (A) 25 kHz, (B) 50 kHz, (C) 100 kHz.

As evident in this figure, with a higher frequency, surface irregularities increase on the surface of the substrates. This enhances the surface topographic properties of the treated substrates and therefore increases the biocompatibility of the titanium [25, 41–43].

Furthermore, with a higher frequency, a larger amount of energy is delivered to the surface of the substrates, and the temperature increase causes more titanium oxide to form across the surface. This is similar to the results observed from the other parameters. Therefore, the substrates treated with a frequency of 100 kHz are expected to show the highest apatite-inducing ability across their surface.

5.1. Biocompatibility assessment

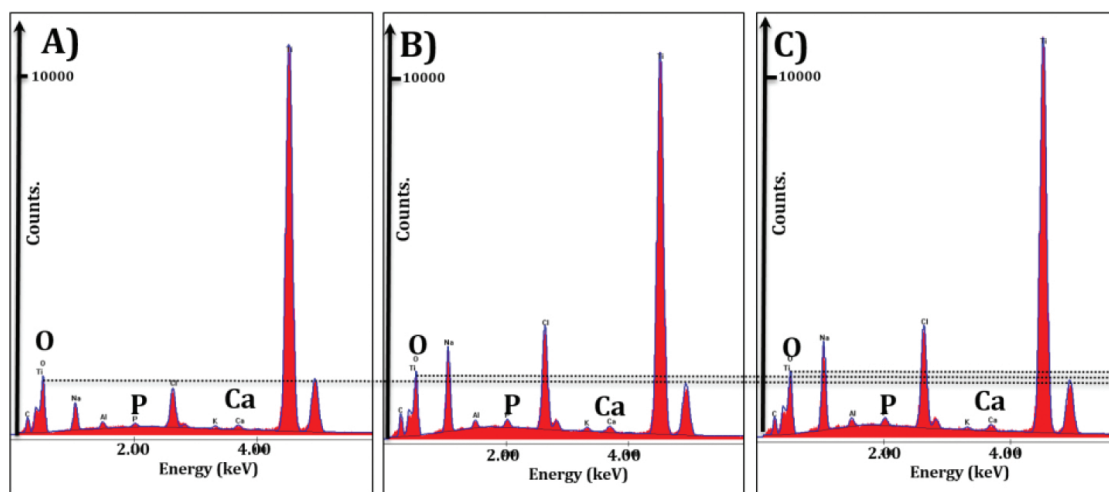**Figure 12** displays the EDX analysis of substrates immersed in SBF for 3 days.

Figure 12. Ti substrates soaked in SBF for 3 days (A) 25 kHz, (B) 50 kHz, (C) 100 kHz.

As evident in **Figure 12**, oxygen concentration slightly increases with an increase in frequency, showing an increase in the concentration of titanium oxide. The higher oxidation level of titanium results in increased negative charge across the surface. Thus, positively charged CO_2, Ca^{2+}, NO_x, and H_2O atoms/ions are attracted to and absorbed by the negatively charged surface of the titanium (OH^-), and create an environment with excellent affinity to biomaterials, such as proteins. The attraction forces between the apatite and the negatively charged titanium oxides are increased through the laser treatment, which, in return, increases the biocompatibility of titanium [25, 42, 43].

This can be further observed by looking at the SEM photography of substrates immersed in SBF.

Figure 13 displays the result.

In this figure, the apatite deposition layer is evident across the irradiated area. As observed from the EDX analysis, the apatite-inducing ability of this substrate is high, which denotes the biocompatibility enhancement of the treated titanium.
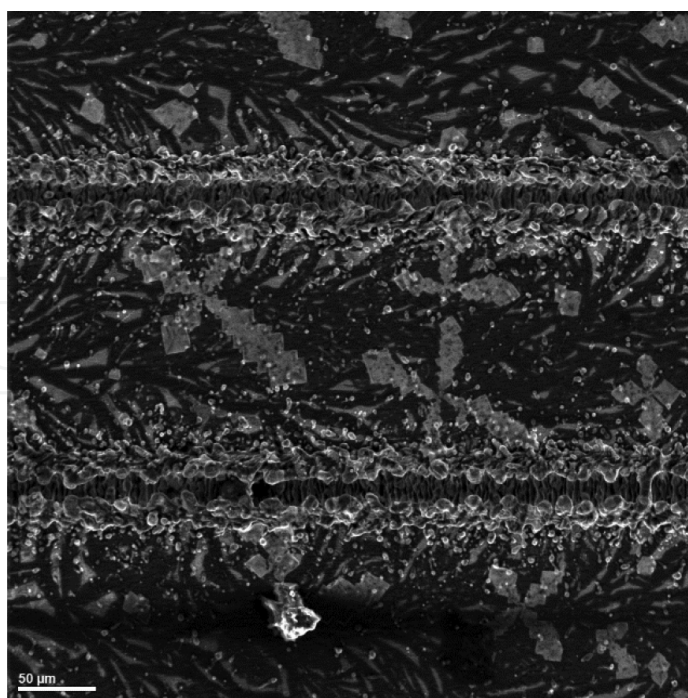
Figure 13. Substrate soaked in SBF for 3 days at 100 kHz.

6. Conclusion

In this chapter, a new method for micro/nano surface texturing of titanium was demonstrated using nanosecond laser irradiation. The application of this method in bone and tissue implant fabrication was explored. Systematic experimental and theoretical studies on effects of the laser parameters on biocompatibility and bioactivity of titanium were conducted. The effects of each parameter were explored individually while other parameters were held constant. Predetermined patterns were induced across thin sheets of titanium substrates to investigate the effects of power, scanning speed, and frequency on surface of the substrates.

Microscopy analysis determined that an increase in power increases the surface topography and ablation across the surface of the material. However, increasing the power within the oxidation limit of titanium can lead to generation of titanium oxide along the irradiation area. Using SBF and cell adhesion, it was found that bioactivity of titanium increases in areas with higher surface topography and higher concentration of titanium oxide.

Additionally, scanning parameters, including pulse number and scanning speed, were found to be influential on the biocompatibility enhancement of titanium substrates. Through a series of experimental and theoretical analysis, it was concluded that a higher pulse number increases the surface energy of titanium substrates, and hence increases the biocompatibility along the irradiation area.

Finally, a range of frequencies was used to examine the bioactivity along the irradiation areas. Microscopy photographs displayed the generation of structures with higher surface topogra-

phy along the laser-induced patterns that have high oxidation and topography properties. Upon biocompatibility assessment, concentrations of calcium, oxygen, and phosphorous are observed on the surface, which shows the bioactivity enhancement of titanium.

This chapter introduced the use of commercially used nanosecond laser systems for biocompatibility enhancement of titanium substrates for fabrication of bone and tissue implants. The key features of this method are described as following:

- Easy controllability

- Simple procedure with rapid processing (single step)

- Feasibility for micro/nano scales

- High efficiency and accuracy

These key features make laser surface texturing desirable for rapid prototyping and fabrication of biomedical devices, and can lead to improvements in cost and durability.

Author details

Amirkianoosh Kiani[*] and Mitra Radmanesh

*Address all correspondence to: a.kiani@unb.ca

Department of Mechanical Engineering, Silicon Hall: Laser Micro/Nanofabrication Facility, University of New Brunswick, NB, Canada

References

[1] Geetha, M., Singh, A. K., Asokamani, R. and Gogia, A. K. (2009). Ti based biomaterials, the ultimate choice for orthopaedic implants–a review. *Progress in Materials Science*, 54(3), 397–425.

[2] Burg, K. J. L.; Porter, S.; and Kellam, J. F. (2000) Biomaterials developments for bone tissue engineering. *Journal of Biomaterials*, 21, 2347–2359.

[3] Geetha, M.; Asokamani, S.; and Gogia, A. K. (2009) Ti based biomaterials, the ultimate choice for orthopaedic implants – a review. *Journal of Progress in Materials Science*, 54, 397–425.

[4] Ponsonnet, L.; Reybier, K.; Jaffrezic, N.; Comte, V.; Lagneau, C.; Lissac, M.; and Martelet, C. (n.d.)., Relationship between surface properties (roughness, wettability) of titanium and titanium alloys and cell behaviour. *Materials Science and Engineering*.

[5] Stevens, M. M. (2008) Biomaterials for bone tissue engineering. *Journal of Materials Today*, 11, 18–25.

[6] Taddei, E. B.; Henriques, V. A. R.; Silva, C. R. M.; and Cairo, C. A. A. (2004) Production of new titanium alloy for orthopedic implants. *Journal of Materials Science & Engineering*, 24, 683–687.

[7] Taimoor H.; Qazi, D.; Mooney, J.; Pumberger, M.; Geißler, S.; and Duda G. N (2015) Biomaterials based strategies for skeletal muscle tissue engineering: existing technologies and future trends. *Journal of Biomaterials*, 53, 502–521.

[8] Gristina, A (1987) Biomaterial-centered infection, microbial adhesion versus tissue integration. *Journal of* Science, 237, 1588–1595.

[9] Wang, H.; Liang, C.; Yang, Y.; and Li, C. (2010) Bioactivities of a Ti surface ablated with a femtosecond laser through SBF. *Journal of Biomedical Materials*, 5, 1–5.

[10] Majumdar, J.; and Manna, I. (2011) Laser material processing. *Journal of International Materials Reviews*, 56, 341–388.

[11] Pereira, A.; Cros, A.; Delaporte, P.; Georgiou, S.; Manousaki, A.; Marine, W.; and Sentis, M. (2004) Surface nano-structuring of metals by laser irradiation: effects of pulse duration, wavelength and gas atmosphere. *Journal of Applied Physics. A.*, 79, 1433–1437.

[12] Ahmmed, T.; Yang, T.; Ling, E. J.; Servio, P.; and Kietzig, A. (2014) Introducing a new optimization tool for femtosecond laser-induced surface texturing on titanium, stainless steel, aluminum and copper. *Journal of Optics and Lasers in Engineering*, 66, 258–268.

[13] Harooni, M.; Carlson, B.; Strohmeier, B. R.; and Kovacevic, R. (2014) Pore formation mechanism and its mitigation in laser welding of AZ31B magnesium alloy in lap joint configuration. *Journal of Materials & Design*, 58, 265–276.

[14] Mukherjee, S.; Dhara, S.; and Saha, P. (2013) Enhancing the biocompatibility of Ti6A14V implants by laser surface microtexturing: an in vitro study. *Journal of International Journal of Manufacturing Technolog*, 76(1–4), 5–15.

[15] Hutmacher, D. W. (2000) Scaffolds in tissue engineering bone and cartilage. *Journal of Biomaterials*. 21, 2529–2543.

[16] Venkatakrishnan, K.; Stanley, P.; Sivakumar, N.R.; Tan, B.; and Lim, L.E.N. (2003) Effect of scanning resolution and fluence fluctuation on femtosecond laser ablation of thin films. *Journal of Applied Physics*, 77, 655–658.

[17] Tong, W. Y., Y. M. Liang, Vivian Tam, H. K. Yip, Y. T. Kao, K. M. C. Cheung, K. W. K. Yeung, and Y. W. Lam. "Biochemical characterization of the cell-biomaterial interface by quantitative proteomics.(2010) Molecular & Cellular Proteomics 9 (10), 2089–2098.

[18] Tran, D. V.; Lam, Y. C.; Zhen, H. Y.; Murukeshan, V. M.; Chai, J. C.; and Hard, D. E. (2005) Femtosecond Laser Processing of Crystalline Silicon."http://dspace.mit.edu/bitstream/handle/1721.1/7449/IMST010.pdf

[19] Yilbas, B. S.; and Al-Aqeeli, N. (2009) Analytical Investigation Into Laser Pulse Heating and Thermal Stresses. *Journal of Optics & Laser Technology*, 41, 132–139.

[20] Kiani, A.; Venkatakrishnan, K.; and Tan, B. (2013) Optical absorption enhancement in 3D silicon oxide nano-sandwich type solar cell. Journal of Optics Express, 22, A120–A131.

[21] Ashby, M. F.; and Easterling, E. K. (1984) The transformation hardening of steel surfaces by laser beams; I. Hypo-eutectoid steels. *Journal of Acta Metallurgica*, 32, 1935–1937.

[22] Ion, J. C.; Scherclift, H. R; and Ashby, M. F. (1992) Diagrams for laser materials processing. *Journal of Acta Metallurgica et Materialia*, 40, 1539–1551.

[23] Kiani, A.; Venkatakrishnan, K.; and Tan, B. (2011) Enhancement of the optical absorption of thin-film of amorphorized silicon for photovoltaic energy conversion. *Journal of Solar Energy*, 85, 1817–1823.

[24] Woodard, p.; and Druden, J. (1998) Thermal analysis of a laser pulse for discrete spot surface transformation hardening. *Journal of Applied Science*, 85, 2488–2496.

[25] Radmanesh M.; Kiani A. (2015) Bioactivity enhancement of titanium induced by Nd: Yag laser pulses. *Journal of applied biomaterials & functional materials*, 0–0.

[26] Kokubo, T.; and Takadama, H. (2006) How useful is SBF in predicting in vivo bone bioactivity?. *Journal of Biomaterials*, 27, 2907–2915.

[27] Aza, De; Fernandez-Pradas, P. N.; and Serra, P. (2004). In vitro bioactivity of laser ablation pseudowollastonite coating. *Journal of Biomaterials*, 25, 1983–1990.

[28] Kurella, A., & Dahotre, N. B. (2005). Review paper: surface modification for bioimplants: the role of laser surface engineering. *Journal of biomaterials applications*, 20(1), 5–50.

[29] Egerton, R. F. (2005) Physical principles of electron microscopy: an introduction to TEM, SEM, and AEM. Springer, 202, New York, USA.

[30] Goldstein, J. (2012) Scanning Electron Microscopy and X-Ray Microanalysis, Springer, ISBN 978-0-306-47292-3, New York, USA.

[31] Albrektsson, T.; and Wennerberg, A. (2004). Oral implant surfaces: part 1 – review focusing on topographic and chemical properties of different surfaces and in vivo responses to them. *International Journal of Prosthodontics*, 17(5).

[32] Brady, J.; Newton, R.; and Boardman, S. (1995) New uses for powder x-ray diffraction experiments in the undergraduate curriculum. *Journal of Geological Education*, 43, 466–470.

[33] Trtica, M; Gakovic, B; Batani, D; Desai, T; Panjan, P; and Radak, B. (2006) Surface modifications of a titanium implant by a picosecond Nd: YAG laser operating at 1064 and 532nm. *Journal of Applied Surface Science*, 253, 2551–2556.

[34] Kiani, A.; Venkatakrishnan, K.; Tan, B.; and Venkataramanan, V. (2011) Maskless lithography using silicon oxide etch-stop layer induced by megahertz repetition femtosecond laser pulses. *Journal of Optics Express*, 19, 10834–10842.

[35] Colpitts, C.; and Kiani, A. (2016). Synthesis of bioactive three-dimensional silicon-oxide nanofibrous structures on the silicon substrate for bionic devices' fabrication. *Journal of Nanomater Nanotechnol*, 6:8. doi: 10.5772/62312

[36] Kiani, A.; Venkatakrishnan, K.; and Tan, B. (2010). Direct laser writing of amorphous silicon on Si-substrate induced by high repetition femtosecond pulses. *Journal of Applied Physics*, 108(7), 074907.

[37] Kiani, A.; Patel, N. B.; Tan, B.; and Venkatakrishnan, K. (2015). Leaf-like nanotips synthesized on femtosecond laser-irradiated dielectric material. *Journal of Applied Physics*, 117(7), 074306.

[38] Radmanesh, M.; and Kiani, A. (2015) ND:YAG laser pulses ablation threshold of stainless steel 304. *Journal of Materials Sciences and Applications*, 6, 634–645, doi: 10.4236/msa.2015.67065.

[39] Gamaly, E. G.; Rode, A. V.; and Luther-Davies, B. (1999). Ultrafast ablation with high-pulse-rate lasers. Part I: theoretical considerations. *Journal of Applied Physics*, 85(8), 4213–4221.

[40] Radmanesh, M.; and Kiani, A. (2015) Effects of laser pulse numbers on surface biocompatibility of titanium for implant fabrication. *Journal of Biomaterials and Nanobiotechnology*, 6, 168–175. doi:10.4236/jbnb.2015.63017.

[41] Zhao, G.; Schwartz, Z.; Wieland, M.; Rupp, F.; Geis-Gerstorfer, J.; Cochran, D. L.; and Boyan, B. D. (2005). High surface energy enhances cell response to titanium substrate microstructure. *Journal of Biomedical Materials Research Part A*, 74(1), 49–58.

[42] Tenner, F.; Brock, C.; Klampfi, F.; and Schmidt, M. (2014) Analysis of the correlation between plasma plume and keyhole behavior in laser metal welding for the modeling of the keyhole geometry. *Journal of Optics and Lasers in Engineering*, 64, 32–41.

[43] Radmanesh, M; and Kiani, A. (2015) "Enhancing biocompatibility of grade 4-titanium using laser surface texturing for bone and tissue transplant applications." 25th Canadian Congress of Applied Mechanics (CANCAM 2015), London, Ontario, Canada.